Nonlinear model predictive control for lifetime extension of self-reconfigurable batteries

Jérôme Blatter, Vincent Heiries, Remy Thomas, Ghislain Despesse

Nonlinear Model Predictive Control for Lifetime Extension of Self-Reconfigurable Batteries

Jérôme Blatter
CEA-LITEN
Univ. Grenoble Aples
F-38000 Grenoble, France
jerome.blatter@cea.fr

Vincent Heiries
CEA-LETI
Univ. Grenoble Aples
F-38000 Grenoble, France
vincent.heiries@cea.fr

Rémy Thomas
CEA-LITEN
Univ. Grenoble Aples
F-38000 Grenoble, France
remy.thomas@cea.fr

Ghislain Despesse
CEA-LETI
Univ. Grenoble Aples
F-38000 Grenoble, France
ghislain.despesse@cea.fr

***Abstract*—Self-reconfigurable batteries (SRB) are advance battery systems where semiconductor switches allow cells to be connected or bypassed dynamically. The in-line configuration even allows the direct generation of AC current without any power converter while allowing a flexible cell usage. This paper introduces a new method of SRB control with nonlinear Model Predictive Control (nMPC) with the aim to reduce battery ageing. A full battery cell model is used to perform the minimization of the SRB capacity losses. Simulation results on WLTP profile validate the proposed method with a capacity loss reduction of 12.4%.**

***Index Terms*—batteries, self-reconfigurable, MPC, optimal control, battery ageing, modelling**

I. Introduction

In a traditional electric vehicle battery pack, cells are statically connected in series and in parallel to comply with voltage and current requirements involving that the weakest cell limits the entire battery pack. Therefore, due to the production process tolerance and different operating conditions in the battery pack, battery cells have capacity and impedance discrepancies, which in addition increase during the battery life [1]. As a consequence, the weakest cell is increasingly limiting [2].

In this context, self-reconfigurable (SRB) batteries are used to deal with the battery pack cell inconstancy. This pack includes switches, allowing to bypass the weakest cell or even to adjust the overall cell layout based on cell's individual state [3]. Therefore, SRB can extract more energy from the cell than traditional battery pack.

In consequence, SRB needs more sophisticated control than the traditional statically series connected battery. In a previous work [4], an accurate nonlinear battery cell model has been developed. Nonlinear Model predictive control (nMPC) appears to be the most appropriate close-loop optimization-based approach due to its ability to control nonlinear systems while taking an objective function and constraints.

This approach is already studied in [5], [6], where nMPC strategy focus on balancing the battery cells capacities and temperature in order to maximize the autonomy and improve the battery ageing due to temperature dispersion. Lifespan increase is therefore an indirect consequence of these controls.

This paper proposes to develop a nMPC which directly optimizes the battery cell capacity loss to demonstrate the full potential of SRB to reduce battery ageing. This study is based on the SRB technology introduced by [7] and illustrated on Fig. 1, where cells are dynamically reconfigured to perform an AC output waveform as represented in Fig. 3. This paper focus on the control of only one phase of the SRB due to a similar control of the three phases.

The proposed approach is validated across a simulation using the power consumption of a car following the Worldwide harmonized Light vehicles Test Procedures (WLTP), which is near the average travelling distance of private vehicles [8]. A Global optimization solution is used as a reference to evaluate the performance of the control regarding the perturbation and the limited length of the MPC prediction horizon.

This paper is organized as follows. In section II, the battery model used for this study is presented. It is similar to the one used in [5] and include an electrical model, a thermal model, a Li-ion cell-ageing model and a SRB reconfiguration model. Section III formulates the optimization problem and describes the nMPC approach. Section IV presents and analyses the results of the previously mentioned simulation. Finally, section V concludes the paper.

II. Battery Model

To perform the optimization in the nMPC control and the simulation, a battery model is required. This is obtained in two steps : first the behaviour of one cell is modelled according to the current circulating through the cell. Then, a SRB model describes the current in each cell depending on the desired output AC signal and the system control vector u.

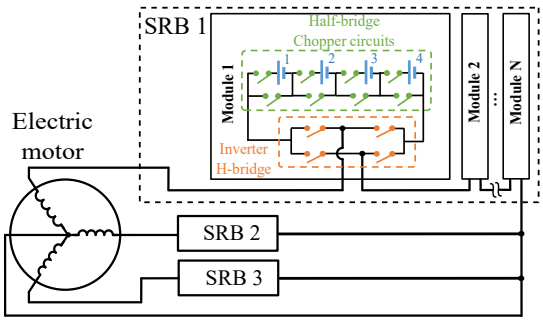

Fig. 1. SRB hardware architecture for an electric vehicle usage

A. Battery cell model

The definition used for State of Charge (SoC), State of Health (SoH) and C_{rate} of a battery cell is given in Eq. (1) to (3).

$$SoC(t) = 100 - \frac{100}{3600(Q_{bol} - Q_{loss}(t))} \int_0^t i_{cell}(\tau)\, d\tau \quad (1)$$

$$SoH(t) = 100\, \frac{Q_{bol} - Q_{loss}(t)}{Q_{bol}} \quad (2)$$

$$C_{rate}(t) = i_{cell}(t)/Q_{nom} \quad (3)$$

with Q_{loss} the cell capacity loss since the beginning of life, i_{cell} the current circulating through the cell, Q_{nom} the cell nominal capacity provided by the manufacturer and Q_{bol} the measured cell capacity at beginning of life. We introduce an initial capacity dispersion model of the cells in a battery pack by a normal distribution of Q_{bol} around Q_{nom}.

For the voltage estimation, a 2-RC Thevenin model (Fig. 2) has been chosen, with $R_1C_1 = 10s$ and $R_2C_2 = 100s$ [4]. The impedances R_j, $j \in \{0, 1, 2\}$ are variable parameters regarding T, SoC, C_{rate} and SoH. So, multi-dimensional cartography obtained by hybrid pulse power characterization at different ageing progression is used to correct cell impedance [3], [4].

The cell thermal dynamic follows a simple heat diffusion model (4). The cells are cooled by the outside at temperature T_{ext} and with the convection rate h_{ext}. C_p is the cell calorific capacity. The thermal power is obtained with the joule effect of the impedances R_j (5) [9]. Reversible heat generation can be ignored [1].

$$C_p\, \dot{T} = P - h_{ext}\, (T - T_{ext}) \quad (4)$$

$$P = R_0\, i_{cell}^2 + \frac{v_{R_1}^2}{R_1} + \frac{v_{R_2}^2}{R_2} \quad (5)$$

Equation (6) represents the degradation function law during cycling [4]. The ageing speed is adapted with the empirical function J dependent of the cell SoC, T and C_{rate} (Fig. 6). α is an ageing accelerating factor when the cell reaches a certain point of capacity loss. A and m are experimental fitting coefficients. An accelerated ageing protocol at different T, SoC and C_{rate} is used to determine the parameters of the model.

$$\dot{Q}_{loss} = \alpha \frac{J(C_{rate}, T, SoC)}{(1 + A\, Q_{loss})^m}\, |i_{cell}| \quad (6)$$

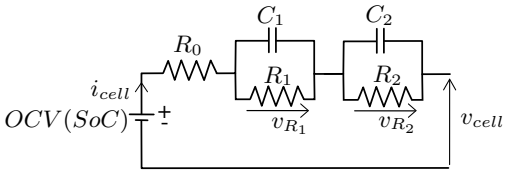

Fig. 2. 2-RC Thevenin Electrical Equivalent Circuit model

B. SRB model

In order to provide an AC waveform, the battery pack follows a reference voltage V_{ref} (7) while supplying a current i_{pack} (8) with U_{rms} the desired output rms voltage, I_{rms} the rms current, θ the signal phase and ϕ the current phase-shift compared to the SRB output voltage.

$$V_{ref}(t) = \sqrt{2}\, U_{rms}(t) \sin(\theta(t)) \quad (7)$$

$$i_{pack}(t) = \sqrt{2}\, I_{rms}(t)\, \sin(\theta(t) + \phi(t)) \quad (8)$$

The battery pack voltage is built by continuously reconnecting the right number of cell in series. As the electric motor operates on a wide frequency range, a relative simple and fast control must be used to calculate the battery pack reconfiguration. Cells do not ensure the same amount of current depending on their connection duration in the staircase sinusoidal voltage illustrated in Fig. 3. In [10], the cell's exchanged current is controlled by connecting them in a specific order in the waveform. Therefore, an average current for each cell can be applied by using a sorting algorithm.

Now, it is assumed that this kind of control is used. The average current flowing through a cell is simplified to (9).

$$i_{cell}(t) = i_{av}(t)\, \mu_{cell}(t) \quad (9)$$

with i_{av} the average current over all cells in one period (11) and $\mu_{cell} \in \mathbb{R}$. The system control vector u reflects the cell utilization rate. This vector is defined as follows with n the number of cells in the battery pack:

$$u = \left(\mu_1 \dots \mu_{cell} \dots \mu_n\right)^T \quad (10)$$

$$i_{av} = \frac{1}{\pi \cdot n} \sum_{cell} \int_0^{\pi} i_{cell}(\theta) d\theta \quad (11)$$

An approximation of i_{av} can be done by considering the use of a FILO strategy (first-in last-out), where a cell is connected and then disconnected once per half period of the AC signal. Thus, i_{av} can be directly computed with (11) from U_{rms}, I_{rms}, ϕ and v_{cell}

It is necessary to constrain the mean value of μ_{cell} to one in order to respect the amount of capacity consumed during utilization. Furthermore, μ_{cell} must be limited concerning the maximal dispersion that the SRB is capable to deal with. A useful dispersion indicator is the stochastic variance. So, μ_{cell}

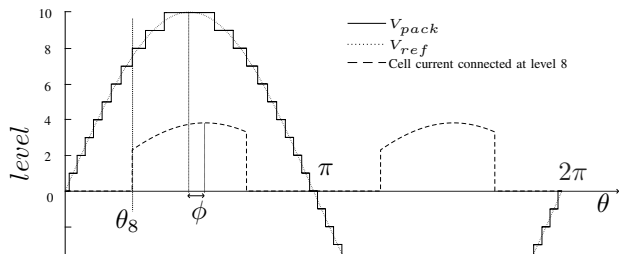

Fig. 3. Staircase waveform generated by SRB

variance must be kept smaller than $\mu_{var\,max}$ the maximal variance that the SRB is capable to manage and must be limited to a lower bound (lb) and an upper bound (ub). Eq. (12) summarizes all constraints on μ_{cell}.

$$\mathbf{C}(u,t) = \begin{cases} \underset{cell}{\text{mean}}(\mu_{cell}) = 1,\ cell \in \{1 \cdots n\} \\ \mu_{cell}(t) \geqslant \mu_{lb}(t) \\ \mu_{cell}(t) \leqslant \mu_{ub}(t) \\ \underset{cell}{\text{var}}(\mu_{cell}(t)) \leqslant \mu_{var\,max}(t) \end{cases} \tag{12}$$

Finally, similarly to the calculation of i_{av}, an average power can be computed for joule effect associated to R_0 :

$$i_{av\,square} = \frac{1}{\pi \cdot n} \sum_{cell} \int_0^{\pi} i_{cell}^2(\theta) d\theta \tag{13}$$

III. Nonlinear Model Prediction Control

Due to errors in the system modelling and unpredictable perturbations, close loop control are needed to correct their outputs according to a measured variable. Additionally, MPC is often used when the control should minimize a cost function over a prediction horizon for a constrained dynamic system. The term nonlinear is added when the cost function is not quadratic and/or the dynamic system is no linear and/or the constraints are not linear.

In this paper, the objective is to develop the nMPC that minimize the capacity loss of the battery while respecting the SRB dynamic and its limits. The SRB capacity loss is defined with the expression $Q_{loss\,pack} = \underset{cell}{\text{mean}}(Q_{loss\,cell})$. Therefore, the following finite horizon optimization problem is formulated as follows:

$$\min_{u(t)} \mathbf{J} = \min_{u(t)} \int_{t_0}^{t_f} t^2\, Q_{loss,\,pack}(t)^2\, dt \tag{14}$$

Subject to :

$$\dot{x}(t) = f(x(t), u(t), I_{rms}(t), U_{rms}(t), \phi(t)) \tag{15}$$

$$2.9 \leqslant v_{cell}(x,t) \leqslant 4.2,\ cell \in \{1 \cdots n\} \tag{16}$$

$$\mathbf{C}(u,t) \tag{17}$$

with $\mathbf{J}$ the cost that must be minimized, t the time variable, x the system's state, f the dynamic system differential function and $t_f - t_0$ the prediction horizon. Applied to the SRB, x is the combined state of every cell in the pack and it is defined as follows: $x = \left(\cdots SoC_{cell} \cdots v_{R1,cell} \cdots v_{R2,cell} \cdots Q_{loss,cell} \cdots T_{cell} \cdots\right)^T$ where $cell \in \{1, \cdots, n\}$. f is defined by the combined dynamic of every cell model presented in section II-A and the average current model of the SRB (11).

In order to return a more convex cost function and easier to solve problem, (14) is a quadratic expression and has a weighting that increase with time.

In the prediction horizon, $I_{rms}(t)$, $U_{rms}(t)$ and $\phi(t)$ are unknown functions and are received as perturbation. Among several techniques that can estimate those functions, constant values is the implemented technique.

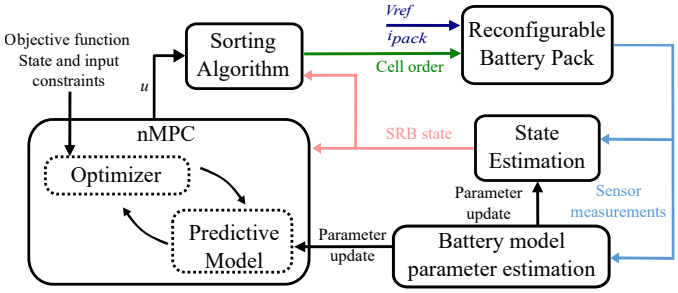

Fig. 4. MPC control loop

For all batteries pack using Li-ion cells, voltage limits of every cell must be respected. This can be included in the optimization problem with the inequality constraint (16). However, because of the perturbation and the error in the system modelling, it is possible that these constraints can not be respected. To avoid a blocking situation in the optimizer, these constraints are modified as penalty function and are added to the cost function.

Finally, this problem is solve with numeric methods. A direct multiple shooting method combined with the SQP algorithm is used [11]. Discretization is performed by solving linear time-variant system for the computation of SoC, T and v. Q_{loss} is solved by performing the Euler method because the time step is chosen small compared to the other four variables. So, the optimal solution is a discrete function : $u(k\,\Delta t \leqslant t < (k+1)\,\Delta t) = u_k | k \in 1, \ldots, K$ with Δt the step time and K the maximal horizon step.

In nMPC control, after computing the optimal solution, only the first action step $u_{k=1}$ is used. Then, this command is provided to the sorting algorithm described in section II and represented with all the control loop in Fig. 4.

IV. Simulation Results

The battery pack chosen for the simulation uses 25 Li-ions cells with $Q_{nom} = 2.9$A.h. The battery cell model is based on Nickel Manganese Cobalt (NMC) 18650 cell with graphite anode [4] and the empirical ageing function is illustrated in 6. Additionally, the battery pack starts to be simulated with a normal distribution for cell's Q_{bol} and R_0, with a standard deviation of respectively 1% and 6% [1]. Battery cell numeration is in the ascending order of the cell's Q_{bol}.

U_{rms}, I_{rms} and ϕ are calculated according to an electric car motor model using a WLTP profile. It is assumed that the electric motor changes from a constant flux control to a constant voltage control at 40 km/h. The maximum voltage of the profile is then adjusted to the voltage that a 25 cells SRB can supply at end of discharge $max(U_{rms}) = \frac{2.9 \cdot 25}{\sqrt{2}}$V.

I_{rms} is adjusted to perform a depth of discharge of 10%. The end of the profile corresponds to a battery charge at $U_{rms} = 44.2$V and $I_{rms} = 3$A until battery SoC reach 90% again. The resulting profiles are illustrated on Fig. 5.

During the discharge profile, the previously described nMPC control is use with the following parameters : $K = 20$,

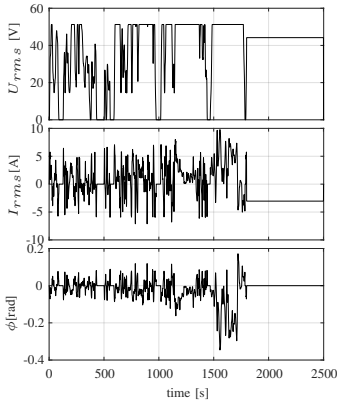

Fig. 5. Cycle profile

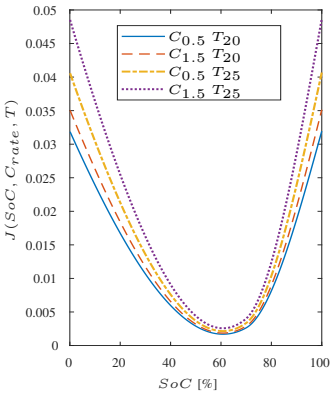

Fig. 6. Ageing speed function

$\Delta t = 10s$. For the prediction process, U_{rms} is a constant value of 44.2 V. I_{rms} and ϕ are kept constant at the last measured value. During the charge profile, U_{rms}, I_{rms} and ϕ are known values. For the 700 last second, an open loop global solution is found using the optimization problem of the nMPC with an additional SoC equalizing constraint for the last step. The simulation result can be viewed on Fig. 7b.

This can be compared to a reference simulation represented in Fig. 7a which is a simulation of the SRB that use the cells in an equalized manner : $\mu_{cell} = 1,\ \forall cell \in \{1 \dots n\}$.

Finally, Fig. 8 shows the simulated $Q_{loss,\,pack}$ of the nMPC and reference simulations. Additionally, the simulation of a $Q_{loss,\,pack}$ resulting of the use of a global solution is represented. This solution is obtained like the open loop global solution in the charge profile of the nMPC simulation but it is applied over all the profile with the absolute knowledge of U_{rms}, I_{rms} and ϕ.

Despite the higher T and C_{rate} for some cells, it can be seen that $Q_{loss,\,pack}$ obtained with the nMPC control is 12.4 % lower than the one in the reference simulation. This is mostly explainable by the fact that ageing speed function, illustrated

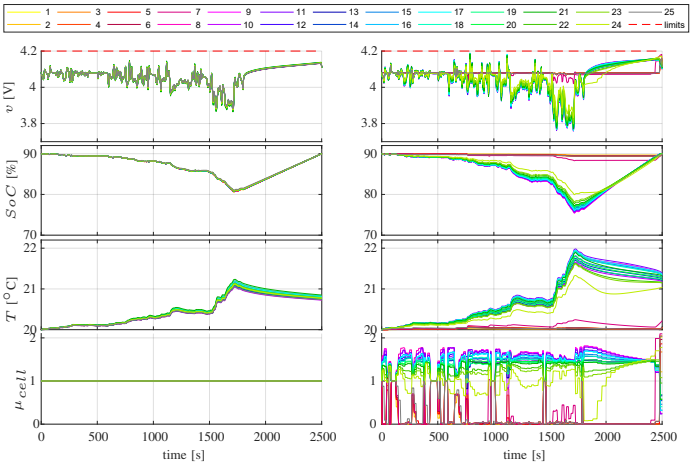

(a) Reference Simulation (b) Simulation using the nMPC

Fig. 7. Simuation of the WLTP profile

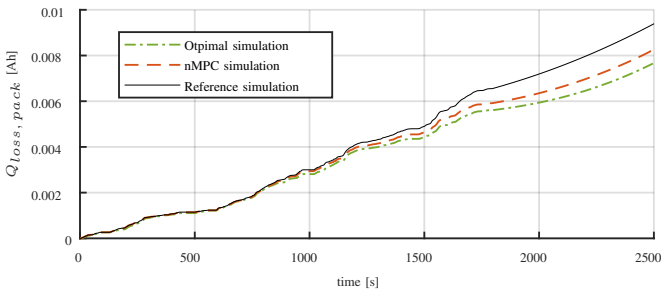

Fig. 8. SRB capacity loss comparative between the reference, the nMPC and the global optimization simulation

in Fig. 6, decrease more with the SoC than for T and C_{rate} for low depth of discharge. Therefore, the nMPC control favours the use of a limited number of cells to decrease their SoC more rapidly.

V. Conclusion

This paper demonstrates the SRB capabilities to reduce battery ageing by using nMPC. A complete battery cell model including cell ageing allows to perform the minimization on the battery capacity loss in a realistic framework. Simulating the nMPC on WLTP profile discharge exhibits a major capacity loss reduction of 12.4%. However, the global optimal solution results show that a reduction of 18.6% is possible. A more sophisticate prediction of the perturbation would certainly bring the nMPC closer to the global optimal.

References

[1] S. Paul, C. Diegelmann, H. Kabza, and W. Tillmetz, "Analysis of ageing inhomogeneities in lithium-ion battery systems," *Journal of Power Sources*, vol. 239, pp. 642–650, 2013.

[2] L. Lu, X. Han, J. Li, J. Hua, and M. Ouyang, "A review on the key issues for lithium-ion battery management in electric vehicles," *Journal of Power Sources*, vol. 226, pp. 272–288, 2013.

[3] Komsiyska and al., "Critical Review of Intelligent Battery Systems: Challenges, Implementation, and Potential for Electric Vehicles," *Energies*, vol. 14, no. 18, p. 5989, Sep. 2021.

[4] A. Laurin, V. Heiries, and M. Montaru, "State-of-Charge and State-of-Health online estimation of Li-ion battery for the More Electrical Aircraft based on semi-empirical ageing model and Sigma-Point Kalman Filtering," in *2021 Smart Systems Integration (SSI)*, Apr. 2021, pp. 1–4.

[5] A. Mondoha, J. Sabatier, P. Lanusse, S. Tippmann, and C. Farges, "Nonlinear Model Predictive Control for a Simulated Reconfigurable Battery Pack," *IFAC-PapersOnLine*, vol. 54, no. 6, pp. 353–358, 2021.

[6] F. Altai, B. Egardt, and L. Johannesson, "Electro-thermal Control of Modular Battery using Model Predictive Control with Control Projections," *IFAC-PapersOnLine*, vol. 48, no. 15, pp. 368–375, 2015.

[7] R. Thomas, G. Despesse, S. Bacquet, E. Fernandez, Y. Lopez, P. Ramahefa-Andry, and L. Cassarino, "A high frequency self-reconfigurable battery for arbitrary waveform generation," *World Electric Vehicle Journal*, vol. 12, no. 1, pp. 1–12, 2021.

[8] E. Paffumi and G. Martini, "Real-World Mobility and Environmental Data for the Assessment of In-Vehicle Battery Capacity Fade," *World Electric Vehicle Journal*, p. 17, 2021.

[9] C. Forgez, D. Vinh Do, G. Friedrich, M. Morcrette, and C. Delacourt, "Thermal modeling of a cylindrical LiFePO4/graphite lithium-ion battery," *Journal of Power Sources*, vol. 195, no. 9, pp. 2961–2968, May 2010.

[10] R. Thomas, F. Lehmann, J. Blatter, G. Despesse, and V. Heiries, "Performance analysis of a novel high frequency self-reconfigurable battery," *World Electric Vehicle Journal*, vol. 12, no. 1, pp. 1–12, 2021.

[11] A. Rao, "A Survey of Numerical Methods for Optimal Control," *Advances in the Astronautical Sciences*, vol. 135, Jan. 2010.